References and Notes

1. C. W. J. Beenakker and H. Van Houten, in *Solid State Physics*, H. Ehrenreich and D. Turnbull, Eds. (Academic Press, San Diego, CA, 1991), vol. 44, pp. 1–228.
2. L. P. Kouwenhoven *et al.*, in *Proceedings of the Advanced Study Institute on Mesoscopic Electron Transport*, L. P. Kouwenhoven, G. Schön, L. L. Sohn, Eds. (Kluwer, Dordrecht, 1997), series E.
3. D. J. Thouless, *Phys. Rev. B* **27**, 6083 (1983).
4. B. Spivak, F. Zhou, M. T. Beal Monod, *ibid.* **51**, 13226 (1995).
5. F. Zhou, B. Spivak, B. L. Altshuler, *Phys. Rev. Lett.* **82**, 608 (1999).
6. P. W. Brouwer, *Phys. Rev. B* **58**, 10135 (1998).
7. L. P. Kouwenhoven *et al.*, *ibid.* **50**, 2019 (1994); L. P. Kouwenhoven *et al.*, *Phys. Rev. Lett.* **73**, 3443 (1994).
8. V. I. Fal'ko and D. E. Khmel'nitskii, *Zh. Eksp. Teor. Fiz.* **95**, 328 (1989) [*Sov. Phys. JTEP* **68**, 186 (1989)]; J. Liu, M. A. Pennington, N. Giordano, *Phys. Rev. B* **45**, 1267 (1992).
9. L. P. Kouwenhoven, A. T. Johnson, N. C. van der Vaart, C. J. P. M. Harmans, C. T. Foxon, *Phys. Rev. Lett.* **67**, 1626 (1991); L. P. Kouwenhoven *et al.*, *Z. Phys. B* **85**, 381 (1991).
10. H. Pothier, P. Lafarge, C. Urbina, D. Esteve, M. H. Devoret, *Europhys. Lett.* **17**, 249 (1992).
11. M. W. Keller, J. M. Martinis, R. L. Kautz, *Phys. Rev. Lett.* **80**, 4530 (1998).
12. M. Büttiker, H. Thomas, A. Prêtre, *Z. Phys. B* **94**, 133 (1994).
13. H. U. Baranger and P. A. Mello, *Phys. Rev. Lett.* **73**, 142 (1994); R. A. Jalabert, J.-L. Pichard, C. W. J. Beenakker, *Europhys. Lett.* **27**, 255 (1994); I. H. Chan, R. M. Clarke, C. M. Marcus, K. Campman, A. C. Gossard, *Phys. Rev. Lett.* **74**, 3876 (1995).
14. Voltages on these gates have a dc component, V_g, and an ac component (at megahertz frequencies) produced by two frequency-locked synthesizers (HP 3325) with a computer-controlled phase difference ϕ between them. To allow a sensitive lock-in measurement of the pumping signal, the ac gate voltages are chopped by a low-frequency (93 Hz) square wave, and the voltage across the dot is measured synchronously with a PAR 124 lock-in amplifier. A bias current can also be applied directly from the lock-in amplifier, allowing conductance to be measured without disturbing the measurement set-up. The current bias is then set to zero to measure pumping.
15. A. G. Huibers, M. Switkes, C. M. Marcus, K. Campman, A. C. Gossard, *Phys. Rev. Lett.* **81**, 1917 (1998).
16. F. Zhou, personal communication.
17. C. M. Marcus *et al.*, *Chaos Solitons Fractals* **8**, 1261 (1997).
18. The line of symmetry is slightly shifted from the "$B = 0$" line determined from the magnet current as a result of offset magnetic fields.

19. We thank B. Altshuler, A. Auerbach, P. Brouwer, A. Morpurgo, B. Spivak, and F. Zhou for useful discussions. We acknowledge support at Stanford from the Army Research Office under contract DAAH04-95-1-0331 and the NSF-Presidential Faculty Fellowship under contract DMR-9629180-1, and at University of California, Santa Barbara, from the Air Force Office of Scientific Research under grant number F49620-94-1-0158 and by QUEST, an NSF Science and Technology Center.

22 October 1998; accepted 6 January 1999

Structural Maturation of Neural Pathways in Children and Adolescents: In Vivo Study

Tomáš Paus,*[1] Alex Zijdenbos,[1] Keith Worsley,[1] D. Louis Collins,[1] Jonathan Blumenthal,[2] Jay N. Giedd,[2] Judith L. Rapoport,[2] Alan C. Evans[1]

Structural maturation of fiber tracts in the human brain, including an increase in the diameter and myelination of axons, may play a role in cognitive development during childhood and adolescence. A computational analysis of structural magnetic resonance images obtained in 111 children and adolescents revealed age-related increases in white matter density in fiber tracts constituting putative corticospinal and frontotemporal pathways. The maturation of the corticospinal tract was bilateral, whereas that of the frontotemporal pathway was found predominantly in the left (speech-dominant) hemisphere. These findings provide evidence for a gradual maturation, during late childhood and adolescence, of fiber pathways presumably supporting motor and speech functions.

Structural maturation of individual brain regions and their connecting pathways is a condition *sine qua non* for the successful development of cognitive, motor, and sensory functions. The smooth flow of neural impulses throughout the brain allows for information to be integrated across the many spatially segregated brain regions involved in these functions. The speed of neural transmission depends not only on the synapse, but also on structural properties of the connecting fibers, including the axon diameter and the thickness of the insulating myelin sheath (*1*). Axons constituting major fiber pathways in the human brain, such as those of the corpus callosum or the corticospinal tract, continue to develop throughout childhood and adolescence. Postmortem studies suggest that axon diameter and myelin sheath undergo conspicuous growth during the first 2 years of life, but may not be fully mature before adolescence (*2*) or even late adulthood (*3*). However, the scarcity of brain specimens makes it difficult to draw definite conclusions about the timetable of myelination during childhood and adolescence. In vivo studies with magnetic resonance imaging (MRI) therefore play a major role in filling this gap. Previous developmental MRI studies have provided evidence for a continuous increase in the overall volume of white matter and the area of the corpus callosum well into adolescence (*4*), but the analytic procedures used in these studies did not allow the investigators to detect changes in specific corticocortical or corticofugal white matter pathways. Here, we report findings obtained with a technique for computational analysis of age-related changes in local white matter signal throughout the brain. Similar techniques have been used in adults to detect subtle regional differences in gray matter signal between healthy subjects and patients with psychiatric or neurological disorders (*5, 6*).

We obtained brain MRI scans of 111 children and adolescents aged 4 to 17 years (*7*). The images were then processed in a fully automatic system that included the following steps: (i) nonlinear transformation of images into standardized stereotactic space to remove global and local differences in the size and shape of the individual brains; (ii) classification of brain tissue into white matter, gray matter, and cerebrospinal fluid; and (iii) blurring of white matter binary masks to generate three-dimensional (3D) maps of white matter "density" (*8*). Using a linear regression model, we correlated the 111 individual maps of white matter density with the subject's age on a voxel-by-voxel basis (*9*).

Regression analysis revealed significant ($t > 5.0$, $P < 0.04$, corrected) age-related increases in white matter density within the left ($t = 8.9$, $r = 0.65$) and right ($t = 8.0$, $r = 0.60$) internal capsule (Fig. 1) and the posterior portion of the left arcuate fasciculus ($t = 6.6$, $r = 0.54$; Fig. 2). The location of the changes in the posterior limb of the internal capsule suggested that the changes involved the corticospinal and, possibly, thalamocortical tracts. Changes in white matter density within the internal capsule were small but consistent, increasing linearly from age 4 to age 17 by about two standard deviations (Fig. 3). The arcuate fasciculus contains fibers connecting frontal and temporal cortical regions involved in speech. It is therefore noteworthy that age-related white matter increases in this pathway reached significance only in the left but not the right hemisphere; the left hemisphere can be assumed to be dominant for speech in the majority of our right-handed subjects (*10*). The mean white matter density

[1]Montreal Neurological Institute, McGill University, 3801 University Street, Montreal, Quebec H3A 2B4, Canada. [2]Child Psychiatry Branch, National Institute of Mental Health, Building 10, Room 6N240, 10 Center Drive, MSC-1600, Bethesda, MD 20892, USA.

*To whom correspondence should be addressed. E-mail: tomas@bic.mni.mcgill.ca

was significantly higher in the left than in the right arcuate fasciculus (paired t test, $t = 2.3$, $P < 0.05$), whereas the variance of age-related changes was lower in the left hemisphere (Fig. 3). In addition to MRI scans, we have also collected several indicators of language skills, including the Vocabulary subscale of the Wechsler Intelligence Scale for Children–Revised (WISC-R) and the Tests of Achievement from the Woodcock-Johnson Psycho-Educational Battery. We carried out multiple regression analyses of these data and, after removing the effect of age, found no significant relations between any of these behavioral measures and white matter densities in the arcuate fasciculus (*11*).

The impressive consistency of the age-related changes found at the level of the internal capsule may be attributable to a relatively high density of fibers funneled through the narrow space between the thalamus and the globus pallidus and, in turn, a high signal-to-noise ratio. It should be pointed out, however, that similar albeit less robust age-related increases in white matter density were detected at different levels along the putative corticospinal tract (Figs. 1 and 4).

The observed changes in white matter density in the internal capsule and the left arcuate fasciculus may reflect age-related increases in the diameter or myelination of the axons forming these fiber tracts. It has been suggested that the diameter of the thickest fibers in the corticospinal tract increases linearly as a function of body height (*12*). Significant shortening of the central conduction time during childhood and adolescence has been observed in the motor pathway of both human and nonhuman primates (*13*). These observations, as well as our findings, are thus consistent with the relatively protracted development of motor skills believed to be dependent on the corticospinal system, namely those requiring fine finger movements (*14*). Faster conduction velocity can facilitate information flow not only by speeding it up but also by allowing for precise temporal coding of high-frequency bursts of neuronal activity (*15*). It has been proposed that processing of speech sounds requires a neural system capable of tracking rapid changes in acoustic input (*16*). Rapid transfer of information to the auditory cortex and beyond would require fast-conducting fiber systems. A recent observation by Penhune *et al.* (*17*) of larger left than right white matter volume in Heschl's gyrus in the adult human brain is consistent with this notion. Moore *et al.* (*18*) examined brain specimens of children aged 5 to 11 years and observed gradual maturation of axons originating in the superficial layers of the auditory cortex; these axons may contribute to corticocortical connections contained in the arcuate fasciculus.

Thus, the age-related increases in white matter density along the arcuate fasciculus observed here may represent a structural correlate of another component of the audiovocal system, namely the corticocortical pathway mediating sensory-motor interactions between the anterior and posterior speech regions. The interruption of the arcuate fasciculus in adulthood causes conduction aphasia, perhaps as a result of the disruption of both feedforward and feedback mechanisms (*19*). The importance of the feedback mechanism is also shown by the presence of significant modulation of neuronal activity in the human and monkey auditory cortex during speech and vocalization, respectively (*20*). The engagement of such feedback mechanisms may facilitate late stages of speech development, requiring a fast bidirec-

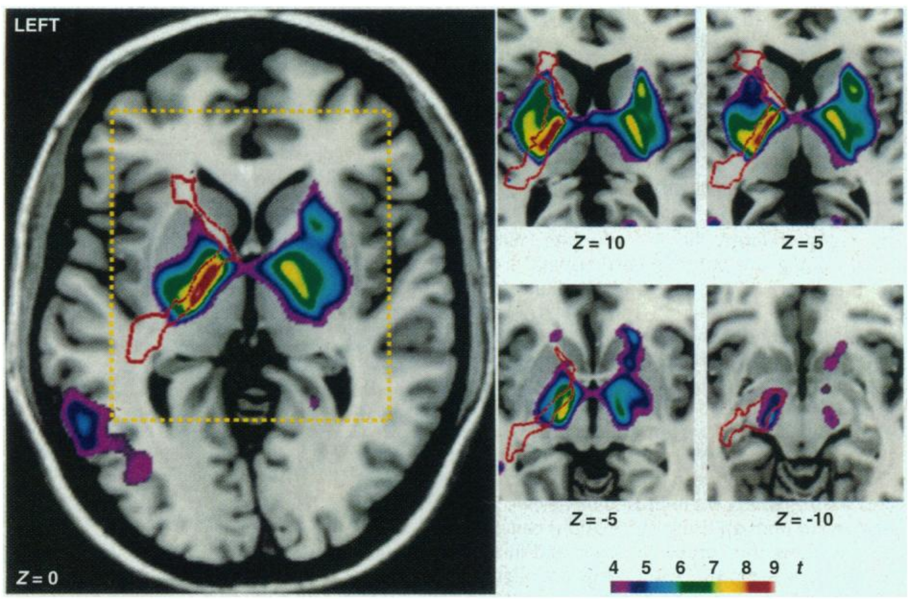

Fig. 1. Age-related changes in white matter density in the internal capsule. The thresholded maps of t-statistic values ($t > 4.0$) are superimposed on axial sections through the magnetic resonance (MR) image of a single subject. The images depict the exact locations in the internal capsule that showed statistically significant correlations between white matter density and the subject's age. The red outline identifies the left internal capsule; its location was derived by registering the MR image with the appropriate sections of the Schaltenbrand and Wahren atlas (*27*). All images are aligned within the standardized stereotactic space, with the Z values indicating the distance (in millimeters) of a given axial section from the horizontal plane passing through the anterior and posterior commissures.

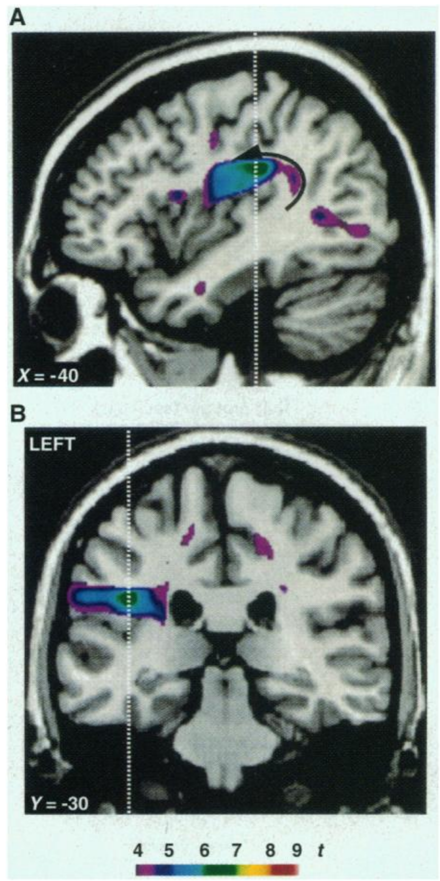

Fig. 2. Age-related changes in white matter density in the left arcuate fasciculus. The thresholded maps of t-statistic values ($t > 4.0$) are superimposed on the sagittal (**A**) and coronal (**B**) sections through the MR image of a single subject. The images depict the locations along the putative arcuate fasciculus that showed statistically significant correlations between white matter density and the subject's age. The t-maps are aligned with the MR image within the standardized stereotactic space, with the X and Y values indicating the distance (in millimeters) from the midline (sagittal section) and the anterior commissure (coronal section), respectively. The dotted line in (A) indicates the level at which the coronal section displayed in (B) was taken and similarly for the dotted line in (B) for the sagittal section displayed in (A).

tional transfer of information between the auditory and motor cortical regions. It is also possible that the age-related increases in white matter density, both along the arcuate fasciculus and the putative corticospinal tract, reflect the effect of extensive use of these systems during the individual's life.

Our findings provide evidence for the protracted structural maturation of fiber pathways, which support motor and speech functions, during childhood and adolescence. Age-related changes in white matter density observed along these pathways may reflect increases in axon diameter, myelination, or concentration of iron, separately or in combination (*21*). Further studies are required to provide a link between the observed MRI-derived structural changes and the speed of neural transmission. This could be achieved, for example, by combining transcranial magnetic stimulation and multichannel electroencephalography (*22*). Our findings may also provide guidance for future investigations of neurodevelopmental disorders such as schizophrenia; the abnormal rate of myelination during childhood or adolescence may very well underlie the emergence of psychotic symptomatology (*23*). Overall, the demonstrated possibility of detecting subtle structural variations in white matter in the living human brain opens up new avenues of research on normal and abnormal cognitive development and the evaluation of long-term effects of various treatment strategies.

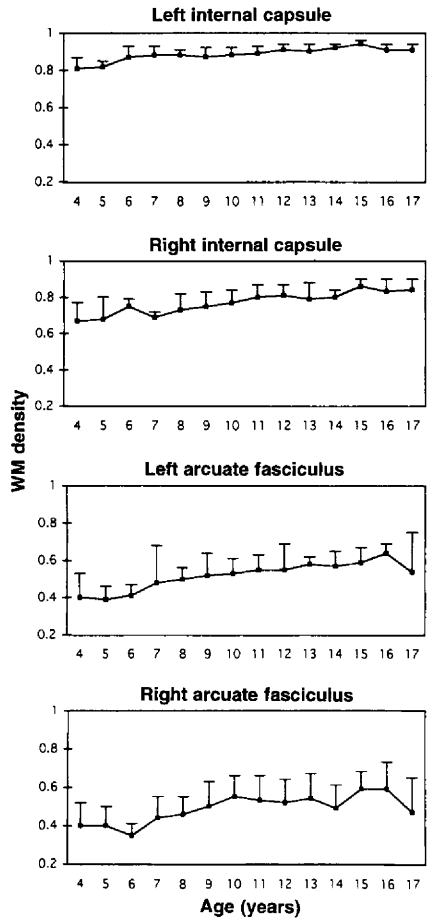

Fig. 3. Values of white matter density in internal capsule and arcuate fasciculus. The plots show means and SDs of white matter density values calculated for each age group. The values were extracted from the individual blurred white matter images at the *X*, *Y*, and *Z* locations corresponding to the voxel with the highest *t* value in a given region, namely in the left internal capsule ($X = -17$, $Y = -12$, $Z = 0$; $t = 8.9$, $r = 0.65$), right internal capsule ($X = 15$, $Y = -4$, $Z = 4$; $t = 8.0$, $r = 0.60$), left arcuate fasciculus ($X = -43$, $Y = -32$, $Z = 26$; $t = 6.6$, $r = 0.54$) and right arcuate fasciculus ($X = 40$, $Y = -25$, $Z = 23$; $t = 4.5$, $r = 0.4$). Numbers of subjects in each age group: 4 years, $n = 7$; 5 years, $n = 10$; 6 years, $n = 3$; 7 years, $n = 5$; 8 years, $n = 12$; 9 years, $n = 10$; 10 years, $n = 7$; 11 years, $n = 11$; 12 years, $n = 7$; 13 years, $n = 10$; 14 years, $n = 10$; 15 years, $n = 8$; 16 years, $n = 7$; and 17 years, $n = 4$.

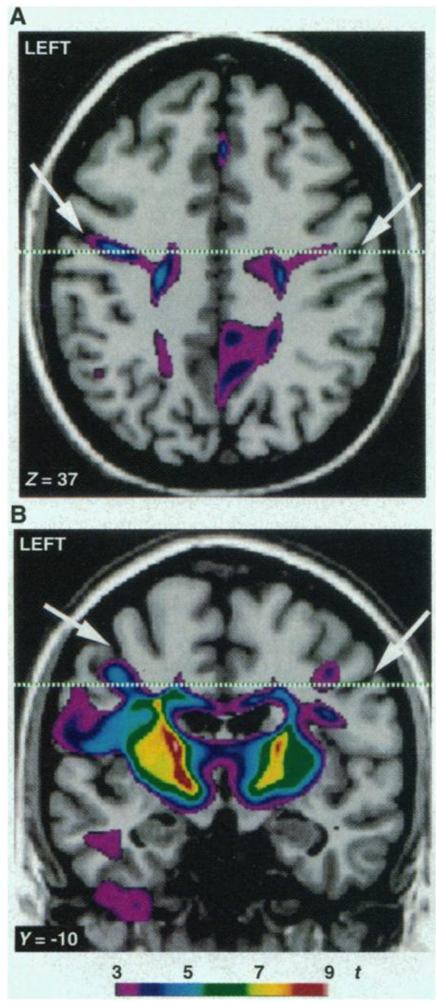

Fig. 4. Age-related changes in white matter density along the putative corticospinal tract. The thresholded maps of *t*-statistic values ($t > 3.0$) are superimposed on the axial (**A**) and coronal (**B**) sections through the MR image of a single subject. The images depict correlations between white matter density and the subject's age along the putative corticospinal tract. Note that the correlations are not limited only to the internal capsule, shown on the coronal section (B), but extend between the capsule and the central sulci, which are indicated by arrows (A). Positive but nonsignificant correlations can also be seen along the corpus callosum and in the left temporal stem (B). The *t*-maps are aligned with the MR image within the standardized stereotactic space, with the *Z* and *Y* values indicating the distance (in millimeters) from the horizontal (axial section) and the vertical (coronal section) planes passing through the anterior commissure, respectively. The dotted line in (A) indicates the level at which the coronal section displayed in (B) was taken and similarly for the dotted line in (B) for the axial section displayed in (A).

References and Notes

1. F. Aboitiz, A. B. Scheibel, R. S. Fisher, E. Zaidel, *Brain Res.* **598**, 143 (1992).
2. J. W. C. Verhaart, *J. Comp. Neurol.* **92**, 1 (1950); P. I. Yakovlev and A. R. Lecours, in *Regional Development of the Brain in Early Life*, A. Minkowski, Ed. (Blackwell Scientific, Oxford, 1967), pp. 3–70; B. A. Brody, H. C. Kinney, A. S. Kloman, F. H. Gilles, *J. Neuropathol. Exp. Neurol.* **46**, 283 (1987); F. M. Benes, *Schizophr. Bull.* **15**, 585 (1989).
3. F. M. Benes, M. Turtle, Y. Khan, P. Farol, *Arch. Gen. Psychiatry* **51**, 477 (1994).
4. White matter: A. Pfefferbaum *et al.*, *Arch. Neurol.* **51**, 874 (1994); A. L. Reiss, M. T. Abrams, H. S. Singer, J. L. Ross, M. B. Denckla, *Brain* **119**, 1763 (1996). Corpus callosum: J. Pujol, P. Vendrell, C. Junque, J. L. Marti-Vilalta, A. Capdevila, *Ann. Neurol.* **34**, 71 (1993); (*24*).
5. N. C. Andreasen *et al.*, *Science* **266**, 294 (1994); F. Vargha-Khadem *et al.*, *Proc. Natl. Acad. Sci U.S.A.* **95**, 12695 (1998).
6. I. C. Wright *et al.*, *Neuroimage* **2**, 244 (1995).
7. Subjects were recruited through local newspaper advertisements and notices (624 responses), then screened by telephone (234 cases excluded) and through mailed questionnaires (another 187 cases excluded). The remaining 203 subjects were brought into the clinic for assessment that included physical, neurological, and psychological examinations [for details see (*24*)]. Individuals with physical, neurological, or lifetime history of psychiatric abnormalities or learning disabilities, or who had any first-degree relatives with major psychiatric disorders, were excluded. The remaining 125 subjects returned for the scanning procedure. Of these, 11 were excluded during scanning (4 with anxiety or claustrophobia, 7 with excessive motion artifact), and 3 others were omitted because of postprocessing failures, so the final sample consisted of 111 subjects. There were 66 boys [age, 10.7 ± 3.8 years (mean ± SD); height, 57.5 ± 9.4 inches; weight, 92.7 ± 41.1 pounds; WISC-R Vocabulary score, 13.3 ± 3.0; WISC-R Block Design score, 13.6 ± 3.0; handedness, 60 (91%) right-handed] and 45 girls [age, 11.5 ± 3.7 years; height, 57.9 ± 8.1 inches; weight, 92.2 ± 35.7 pounds; WISC-R Vocabulary score, 11.8 ± 2.8; WISC-R Block Design score, 11.9 ± 3.7; handedness, 40 (89%) right-handed]. There is a 75% overlap between the sample reported here and that included in our previous studies (*24*) [J. N. Giedd *et al.*, *Cereb. Cortex* **6**, 551 (1996)]. The Institutional Review Board of NIMH approved the protocol. Written consent from the parents and assent from the children were obtained.
8. All MR scans were performed on the same GE Signa 1.5 T superconducting magnet system. In the spoiled-gradient recalled echo 3D acquisition mode, 124 contiguous T_1-weighted (T_R = 24 ms, T_E = 5 ms, flip angle = 45°) 1.5-mm-thick slices were collected in the axial plane. Using the automatic image-processing pipeline [A. P. Zijdenbos, A. Jimenez, A. C. Evans, *Neuroimage* **7**, 783 (1998)], we first transformed the acquired images into standardized stereotactic space in a linear fashion [J. Talairach and P. Tournoux,

Co-planar Stereotactic Atlas of the Human Brain: 3-Dimensional Proportional System. An Approach to Cerebral Imaging (Thieme, Stuttgart, 1988)], followed by nonlinear deformation to match a template brain. These registration procedures are based on an automatic, multiscale feature-matching algorithm [D. L. Collins, C. J. Holmes, T. M. Peters, A. C. Evans, *Hum. Brain Mapp.* **3**, 190 (1995)]. Subsequently, a binary white matter mask was generated for each subject by means of an automatic tissue-classification algorithm. This algorithm is based on classification that uses an artificial neural network classifier (*25*). For each individual T_1-weighted image, we trained the algorithm by providing the stereotactic coordinates of brain regions (voxels) with a minimal 90% likelihood of being gray matter, white matter, or cerebrospinal fluid [A. Zijdenbos *et al.*, *Proceedings of the 4th International Conference on Visualization in Biomedical Computing*, K. H. Hohne and R. Kikinis, Eds. (Springer, Berlin, 1996), pp. 439–448; V. Kollokian, thesis, Concordia University, Montreal (1996)]. The white matter masks obtained in this way were blurred using a Gaussian smoothing kernel (full width at half-maximum, 10 mm); such a smoothing process averages the binary (0 or 1) values of neighboring voxels in 3D space, thus increasing signal-to-noise ratio. The voxel values in the resulting blurred white matter masks are referred to as white matter density (*6*).

9. The data set consisted of 111 pairs of normalized white matter density volumes and age (years) obtained from the 111 subjects. The significance of the relation between age and white matter density was assessed for each of the 3D volume elements (voxels) constituting a volume by means of simple linear regression [R. R. Sokal and F. J. Rohlf, *Biometry* (Freeman, San Francisco, 1981)]. The parameter of interest was the slope of the effect of age on white matter density, after removing the effect of gender. An estimate of the slope and its standard deviation were obtained by least-squares fitting of the linear model at each voxel; *t* values were calculated by dividing the voxel slope-estimate by its standard deviation. The resulting *t*-statistic map tested whether, at a given voxel, the slope of the regression was significantly different from zero. The presence of a significant peak was assessed by a method based on 3D Gaussian random-field theory, which corrects for the multiple comparisons involved in searching across a volume [K. J. Worsley *et al.*, *Hum. Brain Mapp.* **4**, 58 (1996)]. Values equal to or exceeding a criterion of t = 5.0 were considered as significant (df = 108, $P < 0.04$, two-tailed, corrected for whole-brain search).
10. We reanalyzed the data after excluding the 11 left-handed or ambidextrous subjects. The results were not different from those obtained in the original (n = 111) sample.
11. These negative findings should be treated with caution, however. Meaningful correlational analysis of this kind would require administration of a more comprehensive set of neuropsychological tasks known to tap various well-defined brain circuits, such as tests of fine motor skills and phoneme discrimination.
12. J. A. Eyre, S. Miller, V. Ramesh, *J. Physiol.* **434**, 441 (1991).
13. Human subjects: (*12, 26*); K. Muller, V. Homberg, H.-G. Lenard, *Electroencephalogr. Clin. Neurophysiol.* **81**, 63 (1991); A. Nezu *et al.*, *Brain Dev.* **19**, 176 (1997). Monkeys: E. Olivier, S. A. Edgley, J. Armand, R. N. Lemon, *J. Neurosci.* **17**, 267 (1997).
14. D. G. Lawrence and D. A. Hopkins, *Brain* **99**, 235 (1976); H. Forssberg, A. C. Eliasson, H. Kinoshita, R. S. Johansson, G. Westling, *Exp. Brain Res.* **85**, 451 (1991); J. Armand, E. Olivier, S. A. Edgley, R. N. Lemon, in *Hand and Brain: The Neurophysiology and Psychology of Hand Movements*, A. M. Wing, P. Haggard, J. R. Flanagan, Eds. (Academic Press, San Diego, CA, 1996), pp. 125–145; (*26*).
15. W. I. McDonald and T. A. Sears, *Brain* **93**, 583 (1970); H. A. Swadlow, *J. Neurophysiol.* **54**, 1346 (1985); P. Shrager, *Brain Res.* **619**, 278 (1993).
16. P. Tallal, S. Miller, R. H. Fitch, *Ann. N.Y. Acad. Sci.* **682**, 27 (1993); P. Belin *et al.*, *J. Cogn. Neurosci.* **10**, 536 (1998).
17. V. B. Penhune, R. J. Zatorre, J. D. MacDonald, A. C. Evans, *Cereb. Cortex* **6**, 661 (1996).
18. J. Moore, Y. Guan, B. J. Wu, *Assoc. Res. Otolaryngol. Abstr.* **20**, 28 (1997).
19. F. Boller and P. Marcie, *Neuropsychologia* **16**, 521 (1978); A. M. Liberman and I. G. Mattingly, *Cognition* **21**, 1 (1985).
20. P. Muller-Preuss and D. Ploog, *Brain Res.* **215**, 61 (1981); O. Creutzfeldt, G. Ojemann, E. Lettich, *Exp. Brain Res.* **77**, 476 (1989); T. Paus, D. W. Perry, R. J. Zatorre, K. J. Worsley, A. C. Evans, *Eur. J. Neurosci.* **8**, 2236 (1996).
21. Iron contained in oligodendrocytes is believed to play an important role in myelogenesis and the maintenance of myelin sheath [J. R. Conner and S. L. Menzies, *Glia* **17**, 83 (1996)]. Proton magnetic relaxation times are known to vary as a function of iron concentration [J. Vymazal *et al.*, *Magn. Reson. Imaging* **36**, 56 (1996); J. Vymazal, O. Zak, J. W. M. Bulte, P. Aisen, R. A. Brooks, *ibid.*, p. 61] such that a positive correlation can be expected between T_1-weighted signal and iron concentration in a given brain region. In light of the known age-related increases of the non-hemin iron in the human brain [B. Hallgren and P. Sourander, *J. Neurochem.* **3**, 41 (1958)], our findings could also reflect a gradual iron enrichment of white matter oligodendrocytes during childhood and adolescence.
22. R. Ilmonierni *et al.*, *Neuroreport* **8**, 3537 (1997).
23. T. M. Hyde, J. C. Ziegler, D. R. Weinberger, *Arch. Neurol.* **49**, 401 (1992).
24. J. N. Giedd *et al.*, *Dev. Brain Res.* **91**, 274 (1996).
25. M. Ozkan, B. M. Dawant, R. J. Maciunas, *IEEE Trans. Med. Imaging* **12**, 534 (1993).
26. K. Muller and V. Homberg, *Neurosci. Lett.* **144**, 57 (1992).
27. G. Schaltenbrand and P. Wahren, *Introduction to Stereotaxis with an Atlas of the Human Brain, Volume II* (Thieme, Stuttgart, 1977); P. St.-Jean *et al.*, *IEEE Trans. Med. Imaging* **17**, 672 (1998).
28. Supported in part by the International Consortium for Brain Mapping and the Medical Research Council (Canada). We thank G. Leonard, B. Milner, and R. Zatorre for comments on the manuscript and K. Velikonja for help with data analysis.

1 December 1998; accepted 19 February 1999

Signaling of Cell Fate Decisions by *CLAVATA3* in *Arabidopsis* Shoot Meristems

Jennifer C. Fletcher,[1] Ulrike Brand,[2] Mark P. Running,[1*] Rüdiger Simon,[2] Elliot M. Meyerowitz[1†]

In higher plants, organogenesis occurs continuously from self-renewing apical meristems. *Arabidopsis thaliana* plants with loss-of-function mutations in the *CLAVATA* (*CLV1*, *2*, and *3*) genes have enlarged meristems and generate extra floral organs. Genetic analysis indicates that *CLV1*, which encodes a receptor kinase, acts with *CLV3* to control the balance between meristem cell proliferation and differentiation. *CLV3* encodes a small, predicted extracellular protein. *CLV3* acts nonautonomously in meristems and is expressed at the meristem surface overlying the *CLV1* domain. These proteins may act as a ligand-receptor pair in a signal transduction pathway, coordinating growth between adjacent meristematic regions.

The shoot apical meristem (SAM) is the source of all the aerial parts of the plant. Cells at the SAM summit serve as stem cells that divide slowly to continuously displace daughter cells to the surrounding peripheral region, where they are incorporated into differentiating leaf or flower primordia (*1*). A balance between creation of new meristematic cells by division and departure of cells from the meristem by differentiation is required to maintain a functional SAM. The *CLV3* and *CLV1* genes play critical roles in maintaining this balance, because loss-of-function mutations in either gene cause progressive SAM enlargement and floral meristem overgrowth (*2–6*). The phenotypes of representative wild-type and *clv3* mutant plants (*7*) are shown in Fig. 1. *CLV1* encodes a leucine-rich repeat (LRR) transmembrane receptor serine-threonine kinase (*8*). LRRs are a common motif of protein-binding domains (*9*), suggesting that CLV1 may bind an extracellular protein or peptide ligand. *clv1 clv3* double-mutant analysis shows that the genes are mutually epistatic (*5*), suggesting that the two gene products act in the same pathway. Doubly heterozygous (*clv1*/+; *clv3*/+) plants have a *clv* mutant phenotype (*5*), implying that the gene products have a quantitative interdependence, as if they acted together in a complex or in closely associated steps of a pathway. Thus, it appears that CLV3 protein acts either in the intracellular pathway leading from CLV1 activation to cellular activity, or in the production of, or as, the CLV1 ligand.

[1]California Institute of Technology, 1200 East California Boulevard, Pasadena, CA 91125, USA. [2]Institut für Entwicklungsbiologie, Universität zu Köln, Gyrhofstrasse 17, 50923 Köln, Germany.

*Present address: University of California Berkeley, U.S. Department of Agriculture–Agricultural Research Service Plant Gene Expression Center, 800 Buchanan Street, Albany, CA 94710, USA.

†To whom correspondence should be addressed at Division of Biology 156-29, California Institute of Technology, 1200 East California Boulevard, Pasadena, CA 91125, USA. E-mail: meyerow@cco.caltech.edu